


## Genetic evidence for differential functions of *figla* and *nobox* in zebrafish ovarian differentiation and folliculogenesis

Kun Wu <sup>1,2,3</sup>, Yue Zhai<sup>1</sup>, Mingming Qin<sup>1</sup>, Cheng Zhao<sup>1</sup>, Nana Ai<sup>1</sup>, Jianguo He <sup>2,3</sup> & Wei Ge <sup>1</sup>✉

FIGLA and NOBOX are important oocyte-specific transcription factors. Both *figla*<sup>-/-</sup> and *nobox*<sup>-/-</sup> mutants showed all-male phenotype in zebrafish due to increased dominance of the male-promoting pathway. The early diversion towards males in these mutants has precluded analysis of their roles in folliculogenesis. In this study, we attenuated the male-promoting pathway by deleting *dmrt1*, a key male-promoting gene, in *figla*<sup>-/-</sup> and *nobox*<sup>-/-</sup> fish, which allows a sufficient display of defects in folliculogenesis. Germ cells in *figla*<sup>-/-</sup>;*dmrt1*<sup>-/-</sup> double mutant remained in cysts without forming follicles. In contrast, follicles could form well but exhibited deficient growth in *nobox*<sup>-/-</sup>;*dmrt1*<sup>-/-</sup> double mutants. Follicles in *nobox*<sup>-/-</sup>;*dmrt1*<sup>-/-</sup> ovary could progress to previtellogenic (PV) stage but failed to enter vitellogenic growth. Such arrest at PV stage suggested a possible deficiency in estrogen signaling. This was supported by lines of evidence in *nobox*<sup>-/-</sup>;*dmrt1*<sup>-/-</sup>, including reduced expression of ovarian aromatase (*cyp19a1a*) and level of serum estradiol (E2), regressed genital papilla (female secondary sex characteristics), and more importantly the resumption of vitellogenic growth by E2 treatment. Expression analysis suggested Nobox might regulate *cyp19a1a* by controlling Gdf9 and/or Bmp15. Our discoveries indicate that Figla is essential for ovarian differentiation and follicle formation whereas Nobox is important for driving subsequent follicle development.

<sup>1</sup> Department of Biomedical Sciences and Centre of Reproduction, Development and Aging (CRDA), Faculty of Health Sciences, University of Macau, 999078 Taipa, Macau, China. <sup>2</sup> School of Marine Sciences, Sun Yat-sen University, 519082 Zhuhai, China. <sup>3</sup> Southern Marine Sciences and Engineering Guangdong Laboratory (Zhuhai), 519082 Zhuhai, China. ✉email: [weige@um.edu.mo](mailto:weige@um.edu.mo); [gezebrafish@gmail.com](mailto:gezebrafish@gmail.com)

Sex differentiation is the process of gonadal development from bipotential gonads to testis and ovary, which is often initiated by upstream sex-determining factors<sup>1–4</sup>. In the past two decades, evidence has accumulated that both somatic and germ cells play critical roles in sex differentiation and gametogenesis in the differentiated ovary and testis; however, the exact mechanisms and factors involved remain to be elucidated<sup>1,5,6</sup>. Studies in mammals have led to the view that the somatic cells differentiate first in response to sex-determining signals, which in turn program the differentiation of the germ cells into male or female gametes to form testis and ovary, respectively<sup>7–10</sup>. However, this view has been challenged by some studies in fish models. Evidence from both the zebrafish and medaka models suggests important feminizing roles for the germ cells in gonadal differentiation. In zebrafish, germ line deficient fish generated by either mutation of genes specifically expressed in the germ cells such as the *dead end* gene (*dnd*)<sup>11,12</sup> or expression of a cellular toxin in germ cells<sup>12</sup> all developed into males with testis structure, suggesting important roles for germ cells in ovarian differentiation. Similarly, germ cell deficiency induced by morpholino-mediated knockdown or mutation of germ cell-specific genes in medaka fish resulted in sex reversal of genetic females (XX) to males<sup>13,14</sup>. A recent study showed that spermatogenesis could take place in the female gonadal environment (ovary) in the mutant of germ cell-specific *foxl3*, indicating again the importance of germ cell-intrinsic cues for sperm-egg fate decision<sup>15</sup>.

Zebrafish is a well-known model organism in biological, biomedical, and environmental research<sup>6,16–18</sup>. Interestingly, unlike mammals and some other fish species, the domesticated zebrafish strains used in research do not seem to have any master sex-determining genes, such as *Sry* in mammals<sup>19,20</sup>, *dmy/dmrt1Y* in medaka<sup>21,22</sup> and *amhy* in tilapia<sup>23</sup>. The sex of zebrafish is therefore determined by a polygenic mechanism, involving multiple genes<sup>24,25</sup>. The high plasticity of zebrafish gonadal differentiation, which can be influenced by various internal and external factors, makes it an attractive model for investigating the actions and interactions of different factors, including transcription factors such as the factor in the germline alpha (FIGLA) and newborn ovary homeobox gene (NOBOX).

FIGLA and NOBOX are both oocyte-specific transcription factors that play important roles in promoting ovarian development and oogenesis in vertebrates<sup>26–29</sup>. FIGLA was first identified in mice for regulating the expression of zona pellucida genes<sup>29</sup>. Despite being an oocyte-specific factor, the loss of FIGLA in mice did not affect gonadal differentiation at the embryonic stage; however, it caused an arrest of oogenesis at the diplotene stage of meiosis, resulting in failed cyst breakdown and formation of primordial follicles<sup>30</sup>. NOBOX was also discovered in mice, and it played an important role in the formation of primary follicles<sup>26,31</sup>. Similar to FIGLA, the NOBOX null mice also exhibited female infertility with early loss of primary follicles and defective folliculogenesis, exhibiting signs of premature ovarian failure (POF) or insufficiency (POI)<sup>26,32</sup>. Although the expression of NOBOX can be detected in primordial and growing follicles<sup>31,33</sup>, the early defects in folliculogenesis have limited studies on its roles in late stages.

Both FIGLA (*Figla/figla*) and NOBOX (*Nobox/nobox*) have also been studied in teleosts. In medaka, mutation of *figla* caused defects in germ cell cyst breakdown and therefore follicle formation, similar to that of *Figla* knockout (KO) mice<sup>14,27,30</sup>. As for *Nobox*, the follicles in medaka mutant (*nobox*–/–) were arrested at the stage of 300  $\mu$ m-diameter oocytes in the ovary, indicating an essential role for *nobox* in follicle growth<sup>27</sup>. In zebrafish, the loss of *figla* or *nobox* both resulted in all-male offspring<sup>34,35</sup>. In *figla* mutant (*figla*–/–), the oogenesis was blocked early at the

stage of follicle assembly or the transition from cystic prefollicular oocytes at chromatin nucleolar stage (CN, stage IA) to follicular perinucleolar oocytes (PN, stage IB), which was followed by sex reversal to males with normal spermatogenesis, resulting in all-male phenotype<sup>34</sup>. As for *Nobox*, the ovary was extremely underdeveloped in the mutant (*nobox*–/–). In contrast to the *figla* mutant, early PN follicles at the primary growth (PG) stage could occasionally be observed in the *nobox* mutant; however, these follicles failed to develop further to form functional ovaries and all individuals also underwent sex reversal to become males with normal spermatogenesis<sup>35</sup>. Since both *figla* and *nobox* are members of the female-promoting pathway, their loss would disrupt the equilibrium between the male and female-promoting pathways, leading to testis development. As the sex change occurred quickly in female mutants of *figla* and *nobox* before or shortly after ovarian differentiation due to the high plasticity of gonadal differentiation and relatively dominant male-promoting pathway, it is difficult or impossible to characterize their exact functions in controlling folliculogenesis. This has led us to hypothesize that the female-promoting factors such as *figla* and *nobox* could be better studied for their roles in folliculogenesis if the dominance of the male-promoting pathway is alleviated. We have recently tested this idea with aromatase mutant (*cyp19a1a*–/–) by disrupting the male-promoting gene *dmrt1*<sup>36</sup>.

Aromatase (*cyp19a1a*) and doublesex and mab-3-related transcription factor 1 (*dmrt1*) are important for female and male differentiation, respectively. As in other vertebrates, *cyp19a1a* is essential for the production of estrogens in fish<sup>37</sup>, which are important for female gonadal differentiation<sup>38</sup>. On the other hand, *dmrt1* is a critical male-promoting transcription factor essential for testis development and spermatogenesis<sup>39</sup>. As expected, deletion of the *cyp19a1a* gene in the zebrafish resulted in an all-male phenotype whereas the loss of *dmrt1* gene led to a female-biased sex ratio and underdeveloped testis in males<sup>36,40–43</sup>. Interestingly, our recent study showed that simultaneous disruption of *dmrt1* and *cyp19a1a* rescued the all-male phenotype of the *cyp19a1a* mutant in zebrafish and the follicles in the double mutant (*cyp19a1a*–/–;*dmrt1*–/–) could develop well up to the previtellogenic (PV) stage (stage II) with normal formation of cortical alveoli but not yolk granules. This observation suggests that the absence of ovaries in the *cyp19a1a*–/– mutant is likely due to the early and quick diversion of females to males via sex reversal, making it difficult to evaluate the roles of estrogens in follicle development. This discovery reveals that estrogens are not essential for early follicle development including PG-PV transition and subsequent growth of PV follicles, but they are important for late stages of vitellogenic growth<sup>36</sup>. This observation supports our view that the female-promoting factors can be better characterized for their roles in controlling folliculogenesis when the male-promoting pathway is attenuated or blocked to delay or prevent the female-to-male sex reversal.

In this study, we attenuated the male-promoting pathway by disrupting *dmrt1* to study the differential roles of *Figla* and *Nobox* in controlling zebrafish folliculogenesis. We created two double mutants of *figla* and *nobox* with *dmrt1* (*figla*–/–;*dmrt1*–/– and *nobox*–/–;*dmrt1*–/–) with the aim to prevent early female-to-male sex reversal so as to allow *figla*–/– and *nobox*–/– to fully display their developmental defects in ovarian formation and folliculogenesis. Our data provided strong evidence that both *Figla* and *Nobox* play important roles in controlling follicle development; however, they work at different time points of ovarian development and folliculogenesis. *Figla* is mainly involved in controlling cyst breakdown and follicle formation whereas *Nobox* controls subsequent follicle development including follicle activation (primary growth–secondary growth transition) and vitellogenic growth. Furthermore, the oocyte specific transcription factor

Nobox controls vitellogenic growth by regulating aromatase (*cyp19a1a*) expression in the follicle cells, which might be mediated by oocyte-secreted signaling molecules, e.g., Gdf9 and Bmp15.

## Results

**Roles of Figla in follicle formation.** Cyst breakdown or follicle assembly is a critical stage in folliculogenesis<sup>44</sup>. We recently demonstrated in zebrafish that the loss of Figla (*figla*<sup>-/-</sup>) prevented cyst breakdown as no individual follicles could form in the mutant, suggesting an important role for Figla in controlling the transition from the cystic oocytes at prefollicular chromatin nucleolar (CN) stage (stage IA) to individual follicles with perinucleolar (PN) oocytes (stage IB). The mutant showed an all-male phenotype in the end<sup>34</sup>. To further explore the roles of Figla in follicle development, we created a double mutant of *figla* and *dmrt1* genes (*figla*<sup>-/-</sup>;*dmrt1*<sup>-/-</sup>) to prevent early sex reversal.

Histological analysis of gonadal development at 60 dpf showed well-differentiated ovary and testis in the control fish (*figla*<sup>+/-</sup>;*dmrt1*<sup>+/-</sup>) with normal sex ratio and gametogenesis. In *dmrt1* single mutant (*figla*<sup>+/-</sup>;*dmrt1*<sup>-/-</sup>), the sex ratio was biased towards females with normal follicle development; however, the males showed underdeveloped and dysfunctional testis with spermatogenesis blocked at early meiotic stage. As observed previously, all *figla* single mutants (*figla*<sup>-/-</sup>;*dmrt1*<sup>+/-</sup>) were males showing normal spermatogenesis. Interestingly, all double mutant fish (*figla*<sup>-/-</sup>;*dmrt1*<sup>-/-</sup>) had underdeveloped testis identical with the males of *dmrt1* single mutant. Also, the secondary sex characteristics in *figla* and *dmrt1* double mutants (*figla*<sup>-/-</sup>;*dmrt1*<sup>-/-</sup>) were all male-like (with breeding tubercles and without genital papilla) at 60 and 150 dpf (Fig. 1a; Supplementary Fig. 1). Importantly, no follicles could be seen in the gonads of the double mutant at 60 dpf, suggesting failed follicle formation as 60 dpf provided enough time for early follicle formation (Fig. 1). These results suggest that disruption of *dmrt1* could not rescue the female fate of the *figla* mutant as seen with *cyp19a1a* mutant<sup>36</sup>. The gonads could not develop into functional testis or ovary in the absence of *dmrt1* and *figla*, suggesting critical roles for *dmrt1* and *figla* in spermatogenesis and oogenesis, respectively.

**Roles of Nobox in follicle development.** Similar to *figla*, knockout of *nobox*, another oocyte-specific transcription factor, also led to an all-male phenotype in zebrafish<sup>35</sup>. However, in contrast to *figla* whose mutation caused complete failure of follicle formation from the cystic oocytes, the follicles could occasionally form and develop into typical PN follicles at early primary growth (PG) stage in *nobox* mutants (*nobox*<sup>-/-</sup>), more advanced compared to the *figla* mutant (*figla*<sup>-/-</sup>)<sup>34,35</sup>. However, the mutant ovaries were extremely underdeveloped and the follicles failed to grow further. The mutant female fish soon underwent sex reversal to become males<sup>35</sup>. To prevent gonadal masculinization, we created a double mutant with *dmrt1* mutation to block gonadal masculinization.

At 30 dpf, PN follicles of early PG stage could be observed in the gonads of about 50% *nobox* single mutant fish (*nobox*<sup>-/-</sup>;*dmrt1*<sup>+/-</sup>; 5 females/10), similar to the female ratio in the control fish (*nobox*<sup>+/-</sup>;*dmrt1*<sup>+/-</sup>; 5/8, 62.5%); however, compared to the control, the follicles in the *nobox* single mutant were obviously underdeveloped with smaller number and size, suggesting a deficiency in ovarian development (Fig. 2a, b). At 50 dpf, none of the *nobox* single mutant fish contained follicles in the gonads and all fish were males with normal spermatogenesis (11 males/11) as we reported previously<sup>35</sup>, suggesting a quick and early sex reversal from females to males. Interestingly, all double mutant fish (*nobox*<sup>-/-</sup>;*dmrt1*<sup>-/-</sup>) had PN follicles at PG stage

in their gonads (8/8) at 30 dpf and these follicles seemed better developed than those in the *nobox* single mutant. At 50 dpf, the sex ratio of the double mutant fish remained to be female-biased (10 females/12, 83.3%) with well-formed PG follicles in the ovary, in contrast to the all-male phenotype in *nobox* single mutant (Fig. 2c, d); however, the follicles were all arrested at early PG stage without formation of cortical alveoli, in contrast to those in the control and *dmrt1* single mutant (*nobox*<sup>+/-</sup>;*dmrt1*<sup>-/-</sup>) (Fig. 2a, d). These results suggest that the loss of *dmrt1* successfully blocked early sex reversal of *nobox* mutant to males.

To explore the fate of the arrested follicles in the double mutant ovary, we examined the fish at 120 dpf when the control zebrafish were sexually mature with all stages of follicles present in the ovary. Interestingly, we could commonly see follicles that had entered previtellogenic stage (PV, stage II) with abundant cortical alveoli, indicating that the follicles could overcome the arrest and underwent follicle activation (PG-PV transition) in the absence of Nobox (Fig. 3a). This is similar to our observation in the double mutant of *cyp19a1a* and *dmrt1* (*cyp19a1a*<sup>-/-</sup>;*dmrt1*<sup>-/-</sup>), but with a significant delay<sup>36</sup>. What should be noted is that while the follicles could develop to the PV stage, the ovaries of the double mutant were smaller than the well-formed ovaries in *nobox*<sup>+/-</sup>;*dmrt1*<sup>+/-</sup> controls (Fig. 3a, b). The mutant ovaries showed a progressive degeneration with gradual loss of oocytes and a multitude of empty cavities or vacuoles, presumably the remnants of the degenerated or lost oocytes (Fig. 3a, c). The phenotype of oocyte loss was similar to the observation in *Nobox* null mice<sup>26</sup>. The ovarian degeneration was followed by the initiation of sex reversal to males (Fig. 3d). For the convenience of studying and understanding this process, we divided the process of ovarian degeneration in the double mutant into four stages. At Stage I, the ovaries were well formed and structured, containing both PG and PV follicles; however, they were smaller than the control ovaries and contained abundant somatic cells in the interfollicular spaces. Stage II ovaries still contained PG and PV follicles, yet they were markedly smaller in size. At Stage III, the ovaries contained PG follicles only, and at Stage IV, the ovarian tissues had been supplanted by testicular tissues with meiotic cells (Fig. 3).

**Deficiency of estrogen signaling in *nobox* mutant females.** The blockade of follicle development at PV stage with normal formation of cortical alveoli but without yolk accumulation in the double mutant oocytes (*nobox*<sup>-/-</sup>;*dmrt1*<sup>-/-</sup>) raised an interesting question about the involvement of estrogen signaling as estrogen is essential for vitellogenin production and therefore the transition from PV to early vitellogenic (EV) stage<sup>45,46</sup>. To test this hypothesis, we performed a series of experiments.

First, we examined the genital papillae at 100 dpf as this female secondary sex characteristic is estrogen-dependent<sup>47,48</sup>. The genital papillae formed well in control females; however, they were significantly regressed in female double mutants (*nobox*<sup>-/-</sup>;*dmrt1*<sup>-/-</sup>) with shortened lengths (Fig. 4a, b). Second, we assessed the expression of *cyp19a1a* in the ovary and determined the estradiol (E2) concentrations in the serum of double mutant females. Both the mRNA expression of *cyp19a1a* in PV follicles and serum estradiol level were significantly lower in double mutant females (*nobox*<sup>-/-</sup>;*dmrt1*<sup>-/-</sup>) than the control (*nobox*<sup>+/-</sup>;*dmrt1*<sup>+/-</sup>) and *dmrt1* single mutant (*nobox*<sup>+/-</sup>;*dmrt1*<sup>-/-</sup>). There was no significant difference in *cyp19a1a* expression at PG stage, probably because its expression level was very low or barely detectable at this stage<sup>49</sup> (Fig. 4c, d). These lines of evidence indicate that estrogen synthesis was significantly reduced in the double mutant (*nobox*<sup>-/-</sup>;*dmrt1*<sup>-/-</sup>). Third, we created a triple mutant of *nobox*, *cyp19a1a* and *dmrt1* genes (*nobox*<sup>-/-</sup>;*cyp19a1a*<sup>-/-</sup>;*dmrt1*<sup>-/-</sup>).

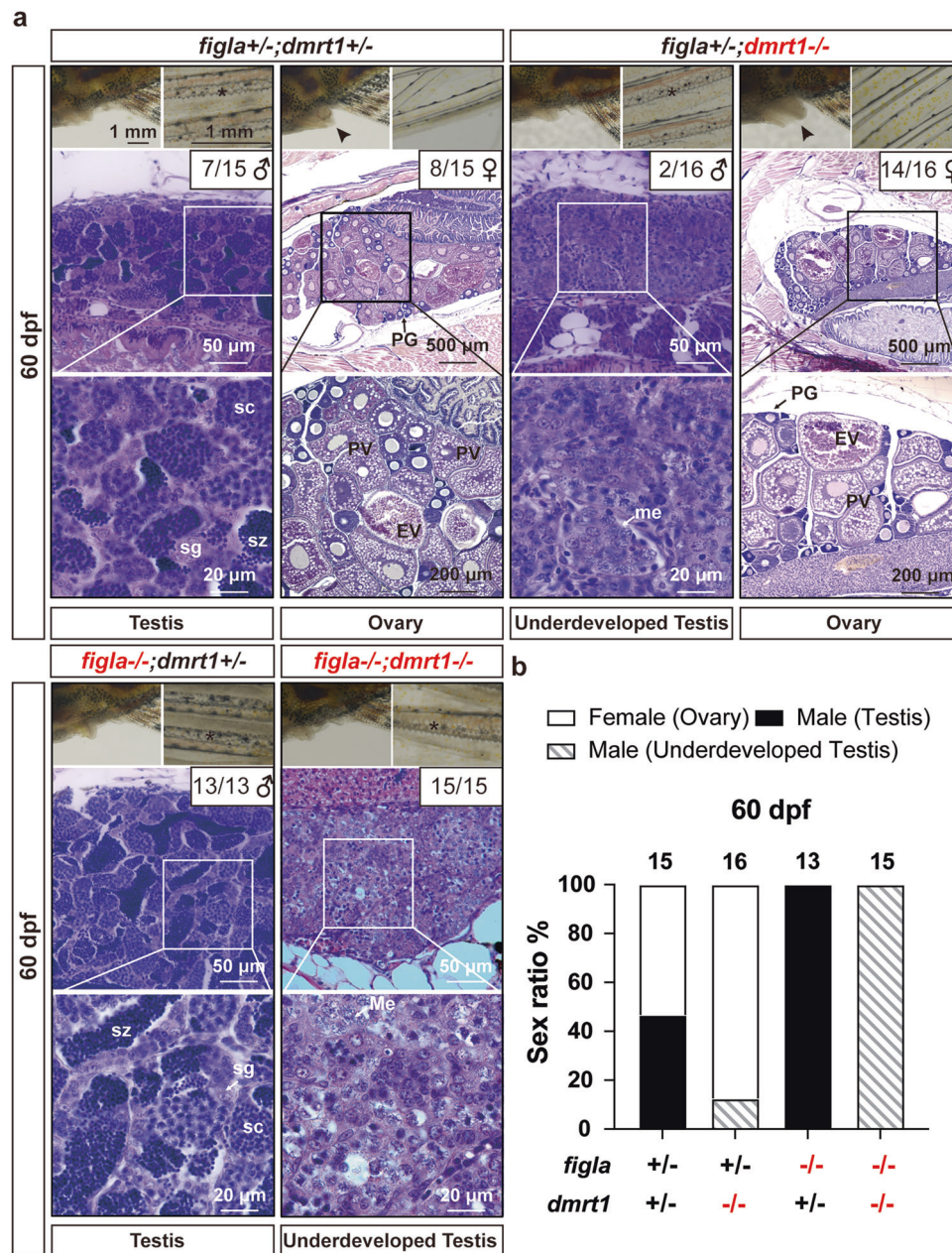


**Fig. 1 Phenotype analysis of different genotypes of *figla* and *dmrt1* mutations at 60 dpf. a** Gonads and secondary sex characteristics of four different genotypes: normal ovary and testis in the control (*figla*<sup>+/-</sup>;*dmrt1*<sup>+/-</sup>; *n* = 15 independent fish, 7 males, 8 females); normal ovary and underdeveloped testis in *dmrt1* single mutant (*figla*<sup>+/-</sup>;*dmrt1*<sup>-/-</sup>; *n* = 16 independent fish, 2 males, 14 females); all-male testis in *figla* single mutant (*figla*<sup>-/-</sup>;*dmrt1*<sup>+/-</sup>; *n* = 13 independent fish, 13 males) and underdeveloped testis in *figla* and *dmrt1* double mutant (*figla*<sup>-/-</sup>;*dmrt1*<sup>-/-</sup>; *n* = 15 independent fish). Asterisk, breeding tubercles on pectoral fins; arrowhead, genital papilla. **b** Sex ratio in four different genotypes at 60 dpf. The sample sizes for independent fish are shown at the top of the columns. PG primary growth, PV previtellogenic, EV early vitellogenic, me meiotic cells, sc spermatocytes, sg spermatogonia, sz spermatozoa.

Compared with *cyp19a1a*<sup>-/-</sup>;*dmrt1*<sup>-/-</sup>, the ovaries from the double and triple mutants containing *nobox*<sup>-/-</sup> (*nobox*<sup>-/-</sup>;*dmrt1*<sup>-/-</sup> and *nobox*<sup>-/-</sup>;*cyp19a1a*<sup>-/-</sup>;*dmrt1*<sup>-/-</sup>) were generally smaller (Fig. 5a, b), which was also reflected in body weight (Fig. 5c). Histological analysis showed that the triple mutant phenocopied the double mutant (*nobox*<sup>-/-</sup>;*dmrt1*<sup>-/-</sup>) at 100 dpf with no additional impact and the follicles could enter PV stage but not vitellogenic stage in both mutants. Although the triple mutant phenocopied the double mutant of *cyp19a1a* and *dmrt1* (*cyp19a1a*<sup>-/-</sup>;*dmrt1*<sup>-/-</sup>) in terms of follicle activation characterized with the formation of cortical alveoli, its ovary was underdeveloped with fewer follicles (Fig. 5b). The mutations of these genes did not seem

to have any pleiotropic effects as no significant difference was observed in body length (Fig. 5d).

Finally, to provide direct and conclusive evidence for the involvement of estrogen signaling in the follicle blockade at PV-EV transition in the double mutant (*nobox*<sup>-/-</sup>;*dmrt1*<sup>-/-</sup>), we performed an experiment to treat both double mutants *nobox*<sup>-/-</sup>;*dmrt1*<sup>-/-</sup> and *cyp19a1a*<sup>-/-</sup>;*dmrt1*<sup>-/-</sup> with E<sub>2</sub>, the major endocrine hormone that promotes vitellogenesis<sup>50</sup>. To avoid the toxic effects of estrogens on follicle development at high dosage<sup>51,52</sup>, we adopted the treatment scheme optimized in our recent study<sup>52</sup>. The fish were treated with E<sub>2</sub> by oral administration of E<sub>2</sub>-containing diet (2 µg/g) for 15 days from 70 to 85

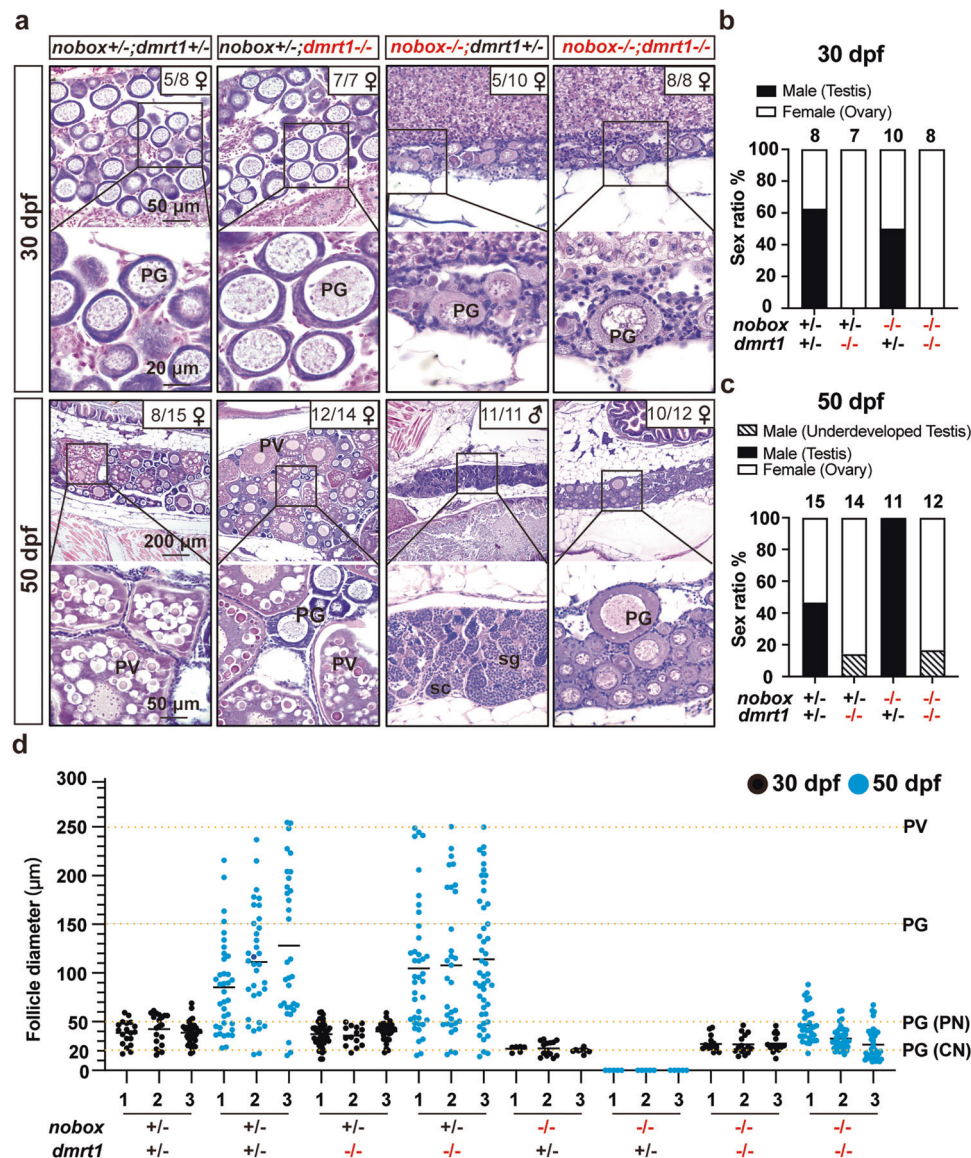


**Fig. 2** Rescue of the all-male phenotype of *nobox* mutant by simultaneous mutation of *dmrt1*. **a** Gonadal histology of *nobox* mutant and double mutant with *dmrt1* mutation in early gonadal differentiation (30 and 50 dpf). **b** Sex ratio in four different genotypes of *nobox* and *dmrt1* mutations at 30 dpf (*nobox* +/-; *dmrt1* +/-:  $n = 8$  independent fish; *nobox* +/-; *dmrt1* -/-:  $n = 7$  independent fish; *nobox* -/-; *dmrt1* +/-:  $n = 10$  independent fish; *nobox* -/-; *dmrt1* -/-:  $n = 8$  independent fish). **c** Sex ratio in four different genotypes of *nobox* and *dmrt1* mutations at 50 dpf (*nobox* +/-; *dmrt1* +/-:  $n = 15$  independent fish; *nobox* +/-; *dmrt1* -/-:  $n = 14$  independent fish; *nobox* -/-; *dmrt1* +/-:  $n = 11$  independent fish; *nobox* -/-; *dmrt1* -/-:  $n = 12$  independent fish). **d** Follicle composition of different genotypes at 30 and 50 dpf ( $n = 3$  independent fish). The horizontal black lines represent the mean. PN perinucleolar oocytes, CN chromatin nucleolar oocytes.

dpf (Fig. 6a). Histological analysis showed that E2 treatment could rescue the PV-EV blockade with yolk accumulation resumed in both double mutants (Fig. 6b). The follicles in the double mutant *cyp19a1a* -/-; *dmrt1* -/- could develop to the full size of FG stage, similar to the follicles in the control fish. In contrast, although vitellogenic growth also resumed in the double mutant *nobox* -/-; *dmrt1* -/-, the follicles could only grow to the range of mid-vitellogenic (MV) stage (Fig. 6c). In agreement with the histological observations, the E2-treated *cyp19a1a* -/-; *dmrt1* -/- females could spawn to produce fertilizable eggs (Fig. 6d) and live offspring (Fig. 6e); however, the E2-treated *nobox* -/-; *dmrt1* -/- females were infertile (Fig. 6d).

**Potential roles of Gdf9 and Bmp15 in mediating Nobox actions.** Nobox is an oocyte-specific transcriptional factor while

estrogens are produced in the surrounding follicle cells by aromatase (*cyp19a1a*)<sup>26,33,53</sup>. This suggests that the reduced expression of *cyp19a1a* in *nobox* mutant must be mediated by other signaling molecules from the oocyte. As growth differentiation factor 9 (GDF9) and bone morphogenetic protein 15 (BMP15/GDF9B) are the two best characterized oocyte-derived growth factors<sup>54</sup> and they both could be regulated by NOBOX in mice<sup>26,55–57</sup>, we hypothesized that these TGF- $\beta$  family members could be potential factors that mediate Nobox regulation of aromatase expression. In support of this idea were recent studies showing downregulation of *cyp19a1a* in *bmp15* null zebrafish<sup>58</sup>. To provide further evidence for the possible involvement of Gdf9 and Bmp15 in Nobox regulation of *cyp19a1a*, we examined the expression of *gdf9* and *bmp15* in the double mutants (*nobox* -/-; *dmrt1* -/-) (no females available in *nobox* single mutant).

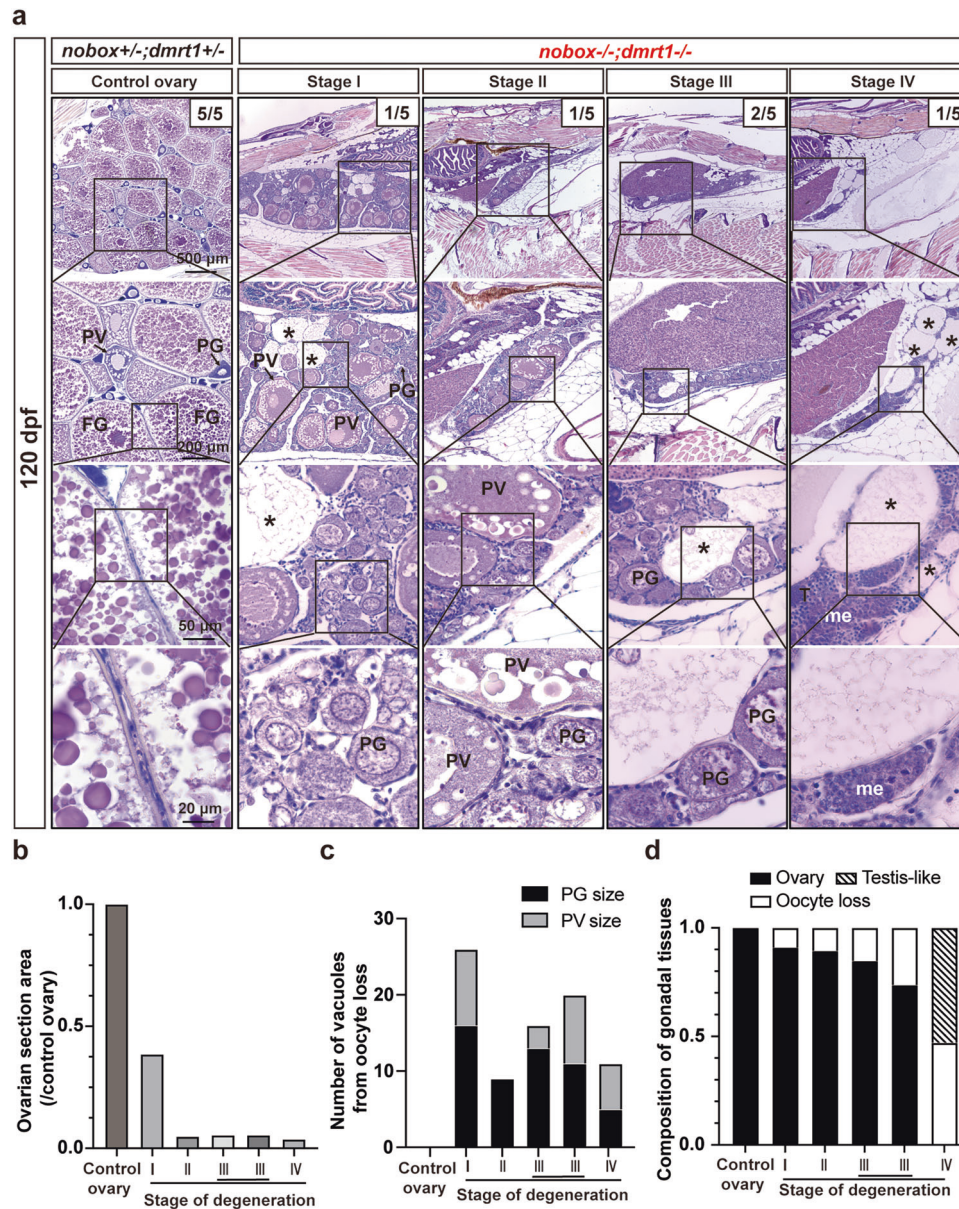


**Fig. 3 Long-term degeneration of the double mutant ovaries.** **a** The ovaries in the double mutant (*nobox*<sup>-/-</sup>;*dmrt1*<sup>-/-</sup>) showed different degrees of degeneration at 120 dpf with loss of oocytes and decreased ovarian size ( $n = 5$  independent fish). In addition, empty cavities or vacuoles left by degenerated oocytes were often observed (asterisks). The degenerated ovaries were gradually replaced by testicular tissues with meiotic cells (me); however, spermatogenesis could not proceed further due to the lack of *dmrt1*. The ovarian degeneration process was categorized into four stages based on gonadal size and morphological features. In stage I, the ovary was significantly smaller than the control (approximately half the size), containing both PG and PV follicles. Stage II was characterized by a dramatically reduced ovarian size, while still housing PG and PV follicles. In stage III, the ovary contained PG follicles only. In stage IV, the ovary was devoid of all follicles, featuring empty cavities or vacuoles left by degenerated oocytes. Additionally, testicular tissues began to emerge with meiotic germ cells. **b** Ovarian sizes of the control and double mutant ovaries undergoing degeneration. The area size of the largest section of each ovary was measured with ImageJ and the data are expressed as the ratios relative to the control. **c** Number of vacuoles resulting from oocyte loss. The vacuoles were counted on the largest section and classified based on their sizes compared to those of PG and PV follicles. **d** Composition of gonadal tissues in the control and double mutant ovaries. The areas of different gonadal tissues were measured using ImageJ.

The results showed that both genes were almost shut off in PG and PV follicles in the absence of *nobox* (*nobox*<sup>-/-</sup>;*dmrt1*<sup>-/-</sup>) compared to the control (*nobox*<sup>+/-</sup>;*dmrt1*<sup>+/-</sup>) and *dmrt1* single mutant (*nobox*<sup>+/-</sup>;*dmrt1*<sup>-/-</sup>) (Fig. 7).

## Discussion

Our previous studies showed that knocking out the oocyte-specific transcription factor *figla* or *nobox* led to an all-male phenotype in zebrafish<sup>34,35</sup>, suggesting crucial roles for these germ cell factors in sex differentiation and gametogenesis,

especially folliculogenesis. The all-male phenotype in *figla* and *nobox* mutants has prevented us from understanding their functions in folliculogenesis due to early differentiation of the juvenile ovary to males. To explore the roles of *figla* and *nobox*, especially their differential roles in folliculogenesis, we weakened the dominance of the male-promoting pathway by deleting *dmrt1* gene, which is essential for male differentiation and spermatogenesis in vertebrates<sup>36,59</sup>. We have successfully used this approach to study ovarian aromatase (*cyp19a1a*), leading to the discovery that *cyp19a1a* and estrogens are essential for ovarian

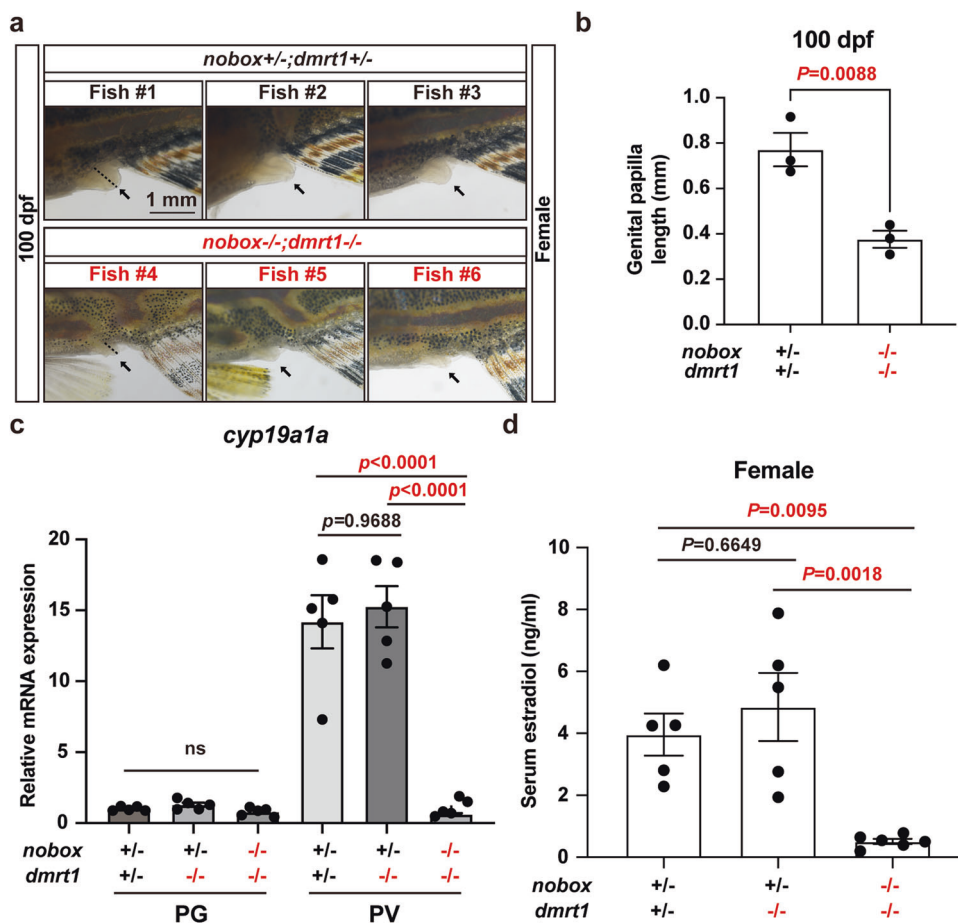


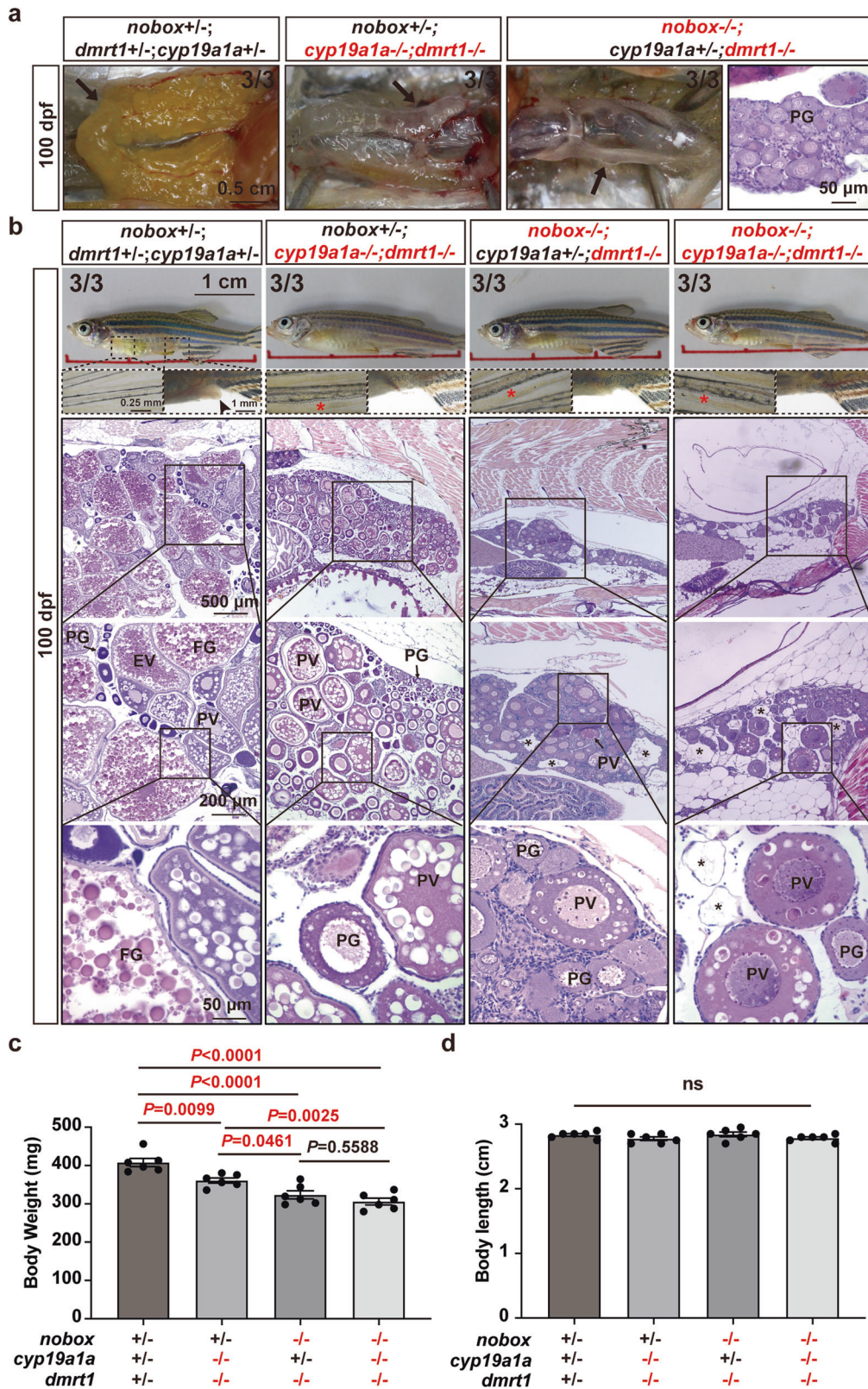
**Fig. 4 Evidence for estrogen deficiency in double mutant females.** **a** Genital papilla in the control (*nobox*<sup>+/-</sup>;*dmrt1*<sup>+/-</sup>; *n* = 3 independent fish) and double mutant (*nobox*<sup>-/-</sup>;*dmrt1*<sup>-/-</sup>; *n* = 3 independent fish) females (arrow). The dotted line showed the length of the genital papilla. **b** Length of genital papilla in the controls and double mutant females (*n* = 3 independent fish). Data shown are mean  $\pm$  SEM ( $P$  = 0.0088 by unpaired Student's two-tailed *t* test). **c** Expression of *cyp19a1a* in PG and PV follicles (*n* = 5 independent samples). Total RNA was extracted from the isolated PG and PV follicles and reverse transcribed into cDNA for real-time PCR analysis. Each data point represents PG or PV follicles isolated and pooled from two fish for each genotype. Data shown are mean  $\pm$  SEM, *P* values revealed by one-way ANOVA and Tukey's test. **d** Serum E2 levels in the control (*nobox*<sup>+/-</sup>;*dmrt1*<sup>+/-</sup>; *n* = 5 independent fish), *dmrt1* single mutant (*nobox*<sup>+/-</sup>;*dmrt1*<sup>-/-</sup>; *n* = 5 independent fish) and double mutant (*nobox*<sup>-/-</sup>; *dmrt1*<sup>-/-</sup>; *n* = 6 independent fish) females at 100 dpf. Data shown are mean  $\pm$  SEM (*nobox*<sup>+/-</sup>;*dmrt1*<sup>+/-</sup> v.s. *nobox*<sup>+/-</sup>;*dmrt1*<sup>-/-</sup>:  $P$  = 0.6649; *nobox*<sup>+/-</sup>;*dmrt1*<sup>+/-</sup> v.s. *nobox*<sup>-/-</sup>;*dmrt1*<sup>-/-</sup>:  $P$  = 0.0095; *nobox*<sup>+/-</sup>;*dmrt1*<sup>-/-</sup> v.s. *nobox*<sup>-/-</sup>;*dmrt1*<sup>-/-</sup>:  $P$  = 0.0018; *P* values revealed by one-way ANOVA and Tukey's test).

differentiation but not for early folliculogenesis from PG to PV stage<sup>36</sup>. Two double mutants were created in the present study (*figla*<sup>-/-</sup>;*dmrt1*<sup>-/-</sup> and *nobox*<sup>-/-</sup>;*dmrt1*<sup>-/-</sup>) for analysis, which has further explored the differential roles of the two transcription factors in controlling folliculogenesis and their action mechanisms, especially Nobox.

Zebrafish is a juvenile hermaphrodite with all individuals forming ovary-like gonads first before developing further into functional ovaries and testes<sup>60</sup>. In the juvenile ovary, the germ cells initiate meiosis to become oocytes at chromatin nucleolar (CN) stage (stage Ia) and in some fish perinucleolar (PN) stage (stage Ib) as well<sup>34,61</sup>. The CN oocytes are clustered in germ cell cysts with synchronous development in each cyst, and some oocytes may develop into PN follicles after the process of cyst breakdown or follicle assembly to become individual follicles. How these events are regulated remains largely unknown. Our recent studies demonstrated that two oocyte-specific transcription factors, Figla and Nobox, played important roles in juvenile ovary to regulate ovarian differentiation and follicle formation.

In *figla*-null zebrafish, the germ cells of CN stage remained in cystic clusters undergoing meiosis; however, these oocyte-like

cells could not form individual follicles, indicating failed cyst breakdown or follicle formation. All mutant fish turned into males quickly, generating an all-male phenotype<sup>34</sup>. Similar to *figla* mutant, the *nobox*-null zebrafish also showed extremely underdeveloped ovaries in juveniles; however, individual follicles of PN stage could occasionally form in the mutant, in sharp contrast to *figla*-null fish. Unfortunately, further assessment of the functional importance of Nobox in regulating subsequent follicle development was not possible due to the early and quick masculinization into males, similar to the *figla* mutant<sup>35</sup>. To evaluate roles especially differential roles of Figla and Nobox in controlling folliculogenesis during and after follicle assembly, we attenuated the male-promoting pathway so as to allow the mutant females of *figla* and *nobox* to fully display their defects in follicle development without early conversion to males. We have used this approach to discover that aromatase (*cyp19a1a*) and therefore estrogens are not essential for the development of follicles from PG to PV stage, in contrast to the traditional views. The loss of *cyp19a1a* gene also resulted in an all-male phenotype with PN follicles occasionally formed in the juvenile ovaries<sup>42</sup>, similar to the *nobox* mutant<sup>35</sup>. Interestingly, the ovary could form normally and folliculogenesis resumed in the double mutant of *cyp19a1a*



and *dmrt1* (*cyp19a1a*<sup>-/-</sup>;*dmrt1*<sup>-/-</sup>), which prevented early sex reversal from females to males<sup>36</sup>.

Using the same approach, we created two double mutant fish in the present study, *figla*<sup>-/-</sup>;*dmrt1*<sup>-/-</sup> and *nobox*<sup>-/-</sup>;*dmrt1*<sup>-/-</sup>, and analyzed their folliculogenesis. The results showed that *figla*<sup>-/-</sup>;*dmrt1*<sup>-/-</sup> exhibited the same phenotype as that seen in the *figla* single mutant (*figla*<sup>-/-</sup>), i.e., cystic CN oocytes without

formation of PN follicles. In contrast, the PN follicles could form adequately in the females of *nobox*<sup>-/-</sup>;*dmrt1*<sup>-/-</sup>. Not only could these follicles develop beyond the PG stage, but they could also progress to the PV stage, marked by the formation of cortical alveoli. This indicates a successful PG-PV transition or follicle activation. Despite these observed follicle developments, the ovaries of the double mutant were significantly smaller than those



**Fig. 5 Ovarian growth and follicle development in the triple mutant of *cyp19a1a*, *nobox* and *dmrt1*.** **a** Gross morphology of the ovaries (arrow) in females of the control (*nobox*+/-;*cyp19a1a*+/-;*dmrt1*+/-, *n* = 3 independent fish), *cyp19a1a* and *dmrt1* double mutant (*nobox*+/-;*cyp19a1a*-/-;*dmrt1*-/-, *n* = 3 independent fish), and *nobox* and *dmrt1* double mutant (*nobox*-/-;*cyp19a1a*+/-;*dmrt1*-/-, *n* = 3 independent fish). **b** Ovarian histology and secondary sex characteristics in different genotypes: control (*nobox*+/-;*cyp19a1a*+/-;*dmrt1*+/-, *n* = 3 independent fish), *cyp19a1a* and *dmrt1* double mutant (*nobox*+/-;*cyp19a1a*-/-;*dmrt1*-/-, *n* = 3), *nobox* and *dmrt1* double mutant (*nobox*-/-;*cyp19a1a*+/-;*dmrt1*-/-, *n* = 3 independent fish), and *nobox*, *cyp19a1a* and *dmrt1* triple mutant (*nobox*-/-;*cyp19a1a*-/-;*dmrt1*-/-, *n* = 3 independent fish). Red asterisk, breeding tubercles; arrowhead, genital papilla; black asterisk, vacuoles left by the lost oocytes. **c, d** Body weight and body length of the triple mutant of *cyp19a1a*, *nobox* and *dmrt1* (*n* = 6 independent fish). Data shown are mean ± SEM, *P* values revealed by one-way ANOVA and Tukey's test.

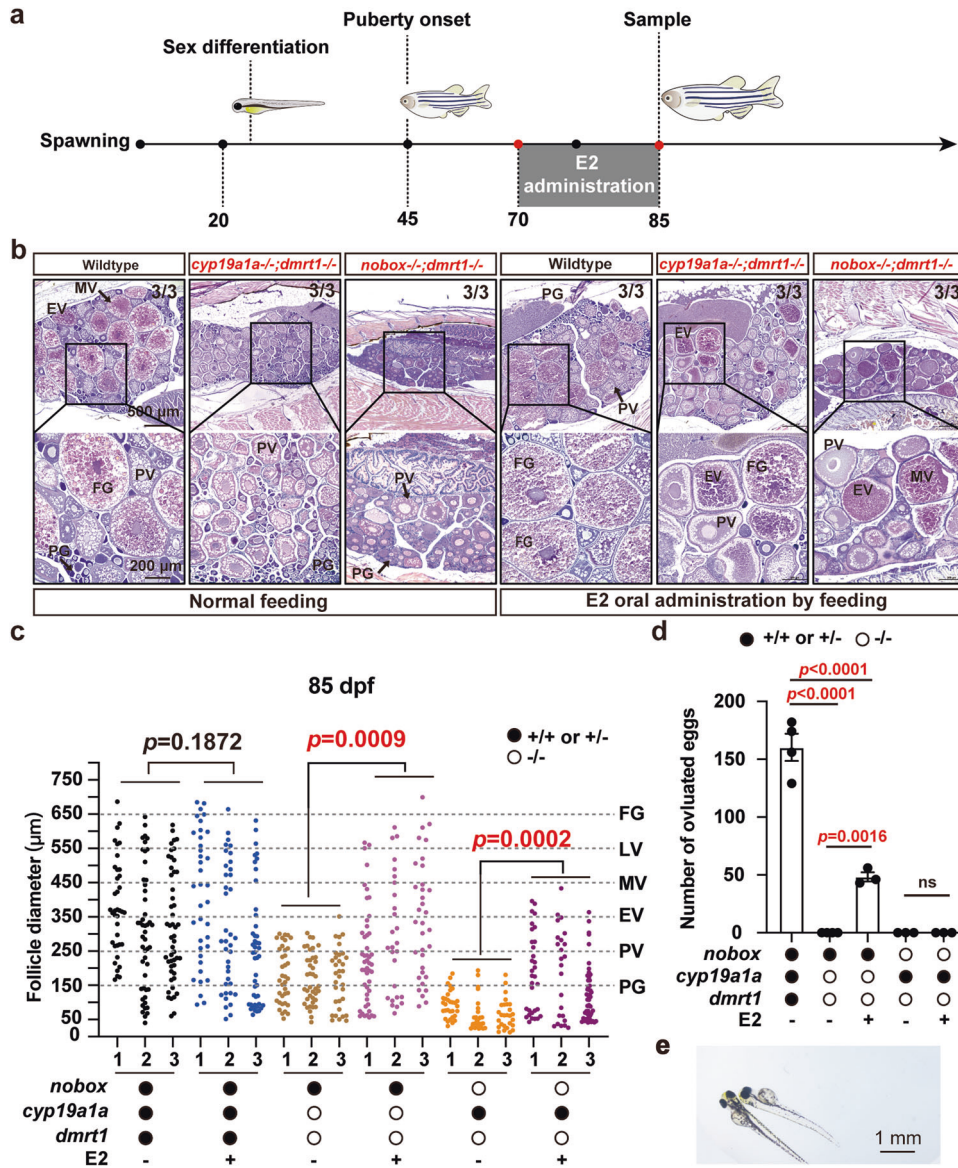


**Fig. 6 Rescue of vitellogenic growth in the double mutants (*nobox*-/-;*dmrt1*-/- and *cyp19a1a*-/-;*dmrt1*-/-) by E2 treatment.** **a** Schematic illustration of E2 treatment. **b** Ovarian histology of different genotypes in the control group with normal feeding and the E2 treatment group fed with an E2-containing diet (*n* = 3 independent fish). Vitellogenic growth characterized with yolk granule accumulation resumed in both double mutants (*nobox*-/-;*dmrt1*-/- and *cyp19a1a*-/-;*dmrt1*-/-), which were blocked at the PV stage with the formation of cortical alveoli but not yolk granules. **c** Follicle composition of different genotypes in different treatment groups (*n* = 3 independent fish). The data points shown are diameters of individual follicles and the statistical significance of the means was demonstrated by unpaired Student's two-tailed *t* test. **d** Fecundity of different genotypes and treatments. Each data point represents the number of eggs spawned by each female mated with one wild-type male (Control group: *n* = 4 independent experiments; Other groups: *n* = 3 independent experiments). The sexes of examined females were further confirmed by histology after mating. Data shown are mean ± SEM, *P* values revealed by one-way ANOVA and Tukey's test. **e** The offspring from E2-treated females of *cyp19a1a*-/-;*dmrt1*-/- double mutant.

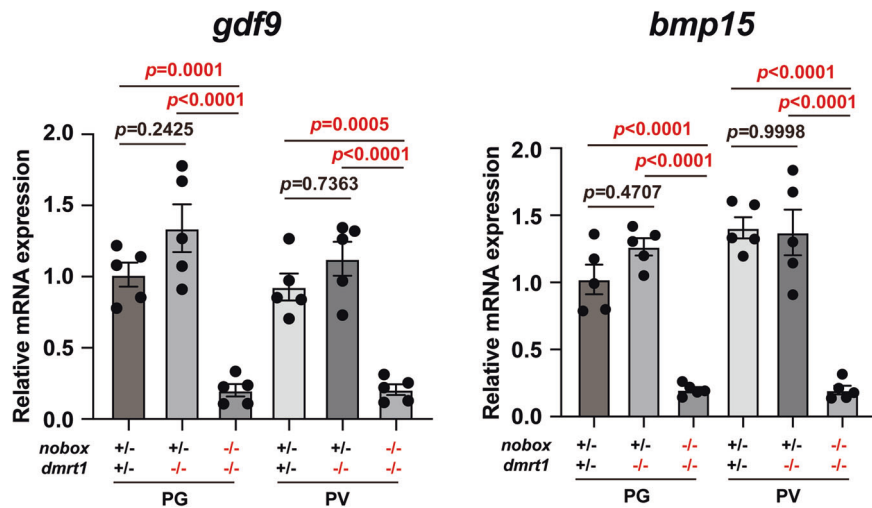


**Fig. 7 Expression of *gdf9* and *bmp15* genes in PG and PV follicles of *nobox*<sup>-/-</sup>;*dmrt1*<sup>-/-</sup> double mutant at 100 dpf.** Total RNA was extracted from the isolated PG and PV follicles and reverse transcribed into cDNA for real-time PCR analysis. Each data point represents PG or PV follicles isolated and pooled from two fish for each genotype, totaling 10 fish ( $n=5$  independent samples). The mRNA levels of each target gene were normalized to that of the housekeeping gene *efla*, and expressed as a fold change relative to the control. Data shown are mean  $\pm$  SEM,  $P$  values revealed by one-way ANOVA and Tukey's test.

of the control, containing far fewer follicles. This reduction may be partially due to a loss of oocytes, as suggested by the presence of numerous vacuoles in the mutant ovaries. These results indicate clearly that *Figla* and *Nobox* are both important for folliculogenesis, albeit at different stages of the process. *Figla* primarily influences cyst breakdown and follicle formation, while *Nobox* acts as a promoter and stabilizer for subsequent progression of follicle development, especially the transition from PV to EV stage. This agrees well with the genetic studies in the mouse model<sup>62,63</sup>, suggesting functional conservation of these oocyte-specific transcription factors in vertebrates. Also, the expression of *Figla* was normal in *Nobox*-null ovary in mice and medaka<sup>26,27</sup> however, no expression of *Nobox* could be detected in the *Figla*-null gonads<sup>27,64</sup>. These results suggest that FIGLA might be an upstream regulator of *Nobox* expression. Alternatively, FIGLA disruption might result in a complete failure of folliculogenesis, therefore preventing *Nobox* expression. More studies are needed in different models to address this issue, including zebrafish.

Interestingly, *nobox*<sup>-/-</sup>;*dmrt1*<sup>-/-</sup> displayed a similar phenotype to that of *cyp19a1a*<sup>-/-</sup>;*dmrt1*<sup>-/-</sup> in that follicles could form and develop to PV stage with normal formation of cortical alveoli. However, the PV follicles in both double mutants could not develop further into the vitellogenic growth phase due to the lack of yolk accumulation. Since vitellogenesis in non-mammalian vertebrates is estrogen-dependent, the similarity between *nobox*<sup>-/-</sup>;*dmrt1*<sup>-/-</sup> and *cyp19a1a*<sup>-/-</sup>;*dmrt1*<sup>-/-</sup> raised an interesting question about the possible involvement of estrogens in *Nobox* regulation of follicle development.

To address this issue, we performed a series of experiments or analyses. First, we determined *cyp19a1a* expression in the ovary and E2 level in the serum. Both decreased significantly in *nobox*<sup>-/-</sup>;*dmrt1*<sup>-/-</sup> females compared to the control fish and *dmrt1*<sup>-/-</sup> single mutant. In agreement with this was the regression of the female secondary sex characteristics, genital papilla, in *nobox*<sup>-/-</sup>;*dmrt1*<sup>-/-</sup> females. The most direct and conclusive evidence for roles of estrogen signaling in *Nobox* actions was the observation that treatment with E2 could rescue the phenotypes of not only *nobox*<sup>-/-</sup>;*dmrt1*<sup>-/-</sup> but also *cyp19a1a*<sup>-/-</sup>;*dmrt1*<sup>-/-</sup>. The PV follicles in both mutants resumed vitellogenesis by accumulating yolk mass in the oocytes in response to E2 supplementation.

Interestingly, although E2 treatment could rescue vitellogenic growth in the double mutant *nobox*<sup>-/-</sup>;*dmrt1*<sup>-/-</sup>, the follicles could only develop maximally to the MV stage, in contrast to the double mutant *cyp19a1a*<sup>-/-</sup>;*dmrt1*<sup>-/-</sup>, whose follicles could develop to the final FG stage in response to E2 and undergo oocyte maturation and ovulation. The blockade of follicle development at MV stage or MV-LV transition in *nobox*<sup>-/-</sup>;*dmrt1*<sup>-/-</sup> after E2 treatment suggests that in addition to regulating *cyp19a1a*, *Nobox* may also control other regulatory factors, which are essential for follicle development beyond the MV stage. The identity of these factors remains unknown. Interestingly, similar follicle arrest at MV stage has also been reported in *bmpr2b* mutant as well as the double mutants *gdf9*<sup>-/-</sup>;*inha*<sup>-/-</sup> and *bmp15*<sup>-/-</sup>;*inha*<sup>-/-</sup><sup>52,65,66</sup>, suggesting potential roles for BMP family members in promoting follicle growth at the MV stage. This would be an interesting issue to explore in future studies.

Since *nobox* and *cyp19a1a* are expressed in two different compartments of the follicle, namely oocyte and follicle cells respectively, it is unlikely that *Nobox* could directly regulate *cyp19a1a* expression. Instead, the regulation is likely mediated by factors secreted by the oocyte. Although the identity of such factors remains unknown, the potential candidates include *Gdf9* and *Bmp15*, which are the two best characterized oocyte-specific growth factors in mammals<sup>54,67</sup>. To provide supportive evidence for this, we examined the expression of *gdf9* and *bmp15* in the ovary of *nobox*<sup>-/-</sup>;*dmrt1*<sup>-/-</sup>. The data showed that the expression of these two genes was almost shut off in the mutant ovary. Further studies are needed to verify their roles in mediating *Nobox* control of *cyp19a1a* expression.

In mammals, *Nobox* has been reported to be a potential transcription factor to regulate the expression of *GDF9* and *BMP15*. Knockout of *Nobox* gene in mice resulted in a complete loss of expression of both *Gdf9* and *Bmp15* together with other oocyte-specific genes<sup>26</sup>. NOBOX binding elements (NBEs) have been identified in the promoter region of mouse *Gdf9* gene and their functionality has been confirmed by luciferase reporter and ChIP assays<sup>56</sup>. As for *BMP15*, although its expression was shut off in *Nobox*-null mice<sup>26</sup>, direct evidence is needed to support NOBOX regulation of *Bmp15* expression at the transcription level. Our data in the present study also implicate *Gdf9* and *Bmp15* in mediating *Nobox* regulation of the follicle cells. Both

genes were significantly downregulated in the double mutant ovary (*nobox*-/-;*dmrt1*-/-). Further evidence for the role of Bmp15 in relaying signals of oocyte specific Nobox to the surrounding follicle cells came from recent studies on *bmp15* in zebrafish. Knockout of zebrafish *bmp15* gene resulted in a complete arrest of follicles at PV stage with normal formation of cortical alveoli but no yolk accumulation<sup>52,58</sup>. Our genetic and pharmacological experiments provided clear evidence that such arrest of follicle development in *bmp15*-null zebrafish was due to reduced expression of *cyp19a1a* and therefore estrogen production<sup>52</sup>. However, more evidence is needed to confirm the regulation of Gdf9 and Bmp15 (or other molecules) by Nobox and their roles in mediating oocyte regulation of follicle cell functions including *cyp19a1a* expression and estrogen biosynthesis (Fig. 8).

In summary, we performed genetic analysis for roles of oocyte-specific transcription factors *figla* and *nobox* in zebrafish folliculogenesis. By attenuating the male-promoting pathway via deleting *dmrt1* gene, we were able to evaluate the functions of both *Figla* and *Nobox* in controlling folliculogenesis without being interrupted by early sex reversal to males. Our data confirmed that *Figla* is essential for germ cell cyst breakdown or follicle assembly whereas *Nobox* is important for the subsequent progression of follicle development, especially the transition from previtellogenic stage to vitellogenic growth (PV-EV transition). We provided further evidence that the *Nobox*-dependent vitellogenic growth was due to a deficiency in estrogen production.

This study has provided strong evidence in a fish model for the important roles of oocyte in orchestrating folliculogenesis (Fig. 8).

## Methods

**Animal.** The mutant zebrafish lines for *cyp19a1a* (*umo5*), *figla* (*umo14*), *dmrt1* (*umo15*), *nobox* (*umo36*) were produced in our previous studies<sup>34–36,42</sup>. The fish were reared at  $28 \pm 1$  °C with a photoperiod of 14-h light and 10-h dark in a flow-through aquarium system (Tecniplast, Buguggiate, Italy). The larvae were reared in nursery tanks with paramecia and artemia before transfer to the aquarium system, and the adults were fed with artemia and Otohime fish diet (Marubeni Nisshin Feed, Tokyo, Japan). Zebrafish husbandry and all experiments were conducted in full accordance with animal care and use guidelines with ethical approval by the Research Ethics Committee of the University of Macau (Approval. No. AEC-13-002).

**Genotyping.** Genomic DNA from an embryo or a small piece of the caudal fin was extracted by alkaline lysis<sup>68</sup>. The sample was incubated in 30–50  $\mu$ l NaOH (50 nmol/ $\mu$ l) at 95°C for 10 min to extract the genomic DNA. Then, 3–5  $\mu$ l Tris-HCl (pH 8.0) was added for neutralization. The extract was used for high-resolution melting analysis (HRMA), and the melt curves were analyzed with the Precision Melt Analysis software (Bio-Rad, Hercules, CA)<sup>68</sup>. The primers used for genotyping are listed in Supplementary Table 1.

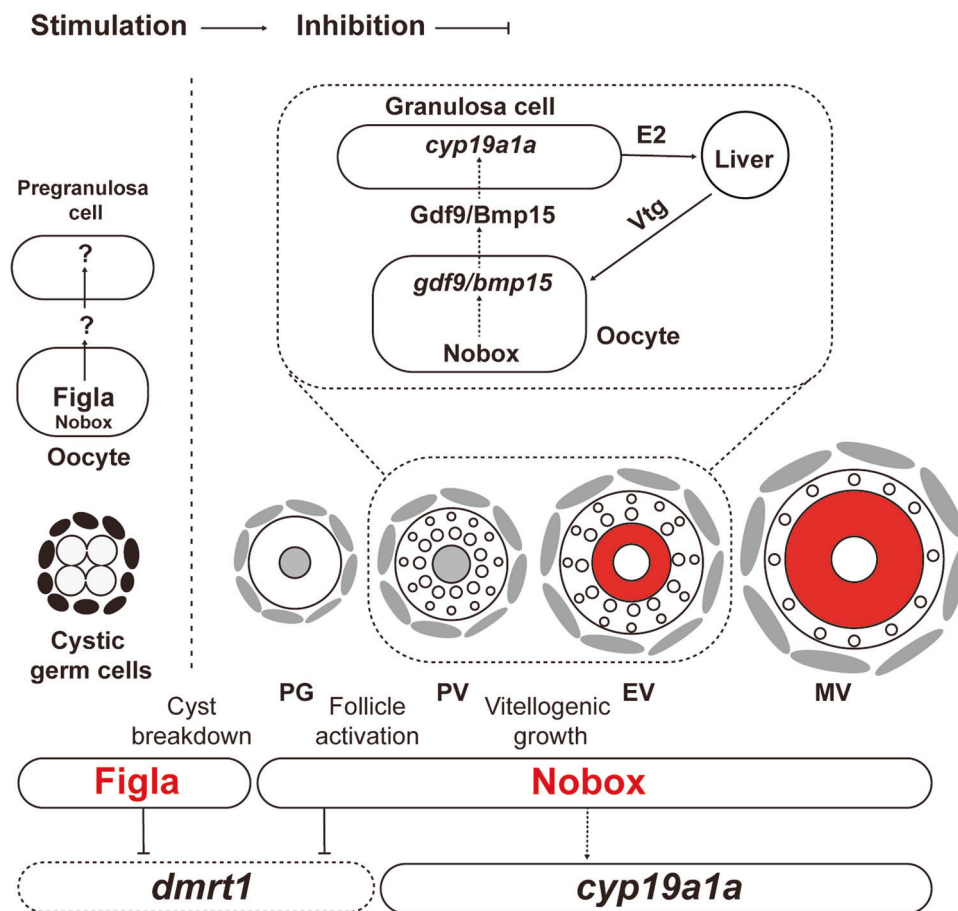


**Fig. 8 A working model on differential roles of *Figla* and *Nobox* in zebrafish folliculogenesis.** *Figla* plays a critical role in controlling follicle formation in the event of cyst breakdown or follicle assembly, while *Nobox* is more involved in regulating follicle development after its formation, including such events as follicle activation (PG-PV transition) and vitellogenic growth (PV-EV transition). *Nobox* controls vitellogenic growth by regulating aromatase (*cyp19a1a*) expression in the follicle cells, which may be mediated by oocyte-secreted signaling molecules such as Gdf9 and Bmp15.

**Sampling and histological examination.** The fish were sampled at different time points for phenotype analysis. The fish were sacrificed after anaesthetization with MS222 (Sigma, St. Louis, MO). The gross morphology of each fish was photographed with a digital camera (Canon EOS 700D). The pectoral fins and cloaca of each sampled fish were examined on the Nikon SMZ18 dissecting microscope (Nikon, Tokyo, Japan) for breeding tubercles and genital papilla and photographed with the Digit Sight DS-Fi2 camera (Nikon).

For histological analysis, the entire fish were fixed in Bouin's fixative for at least 24 h. Dehydration and infiltration were then performed on the ASP6025S Automatic Vacuum Tissue Processor (Leica, Wetzlar, Germany). The samples were embedded with paraffin, followed by serial sectioning at 5  $\mu\text{m}$ . The sections were stained with hematoxylin and eosin (H&E) and viewed on the ECLIPSE Ni-U microscope (Nikon). The photos were taken with the Digit Sight DS-Fi2 camera (Nikon). Sibling wild type (+/+) and/or heterozygous (+/−) fish were used as controls for phenotype analysis.

**Follicle staging.** Follicles were staged according to size and morphological features such as cortical alveoli and yolk granules as reported<sup>69–71,72</sup>. We divide follicles into six stages: primary growth (PG, <150  $\mu\text{m}$ ), previtellogenic (PV, ~250  $\mu\text{m}$ ), early vitellogenic (EV, ~350  $\mu\text{m}$ ), mid-vitellogenic (MV, ~450  $\mu\text{m}$ ), late vitellogenic (LV, ~550  $\mu\text{m}$ ) and full-grown (FG, >650  $\mu\text{m}$ ).

**Fertility assessment.** Female fertility was assessed by the number of eggs spawned in natural breeding with males. The female fish from different groups were paired with wild-type (+/+) males individually for natural spawning. After spawning in the morning, the number of eggs released by each female was counted.

**Sex identification.** In general, the sex was identified according to dimorphic morphological features, such as body shape, fin color, and genital papilla<sup>73</sup>, and, if necessary, by dissection under the Nikon SMZ18 stereomicroscope (Nikon). The sex identity was confirmed by histology at the end of sampling.

**RNA extraction and quantitative real-time PCR.** Total RNA was extracted from isolated PG and PV follicles<sup>74</sup> using TRIzol (Invitrogen, Waltham, MA) according to the manufacturer's protocol. Reverse transcription was performed using M-MLV reverse transcriptase (Invitrogen). Real-time PCR was performed on the CFX384 Real-Time System (Bio-Rad) using primers listed in Supplementary Table 1. Melting curve analysis was performed to demonstrate primer specificity. A standard curve was included in each PCR assay for quantification. The relative gene expression level was normalized to the level of *efla* in each sample and expressed as fold change compared to the control group.

**Measurement of serum E2.** After anaesthetization with MS222, the blood was gently collected from the heart of each fish using a 10- $\mu\text{L}$  tip and transferred into a 1.5-mL tube. The samples were left at room temperature for 1 h to separate the serum. The supernatants were collected after centrifugation (3000 rpm, 30 min, 4 °C). The levels of E2 in the serum were measured using an ELISA kit (Neogen Corporation, Lansing, MI; RRI-D:AB\_2935669) according to the manufacturer's instructions.

**Oral administration of E2.** Different groups of females were treated with E2 for 15 days from 70 to 85 dpf. In brief, the fish were fed twice a day with the E2-containing Otohime fish diet

(0 or 2  $\mu\text{g/g}$ ), each at 5% of the total body weight in the tank (10% per day in total). During the treatment period, the water was renewed daily to maintain good water quality.

**Statistics and Reproducibility.** All values are presented as the mean  $\pm$  sem. The data were statistically analyzed by Student's t-test or one-way ANOVA using Prism 9 (GraphPad Prism, San Diego, CA). The significance is shown by the *P* value in the figures (*P* > 0.05 or ns, not significant). The sample sizes represent independent biological replicates. All experiments were performed at least twice.

**Reporting summary.** Further information on research design is available in the Nature Portfolio Reporting Summary linked to this article.

### Data availability

Original data generated or analyzed during this study are included in this published article or in the data repositories listed in References. Supplementary Data 1 contains all individual data values plotted in the figures, whereas Supplementary Table 1 contains all primers used in this study.

Received: 12 June 2023; Accepted: 7 November 2023;

Published online: 21 November 2023

### References

- Nagahama, Y., Chakraborty, T., Paul-Prasanth, B., Ohta, K. & Nakamura, M. Sex determination, gonadal sex differentiation, and plasticity in vertebrate species. *Physiol. Rev.* **101**, 1237–1308 (2021).
- Bachtrog, D. et al. Sex determination: why so many ways of doing it? *PLoS Biol.* **12**, e1001899 (2014).
- Cutting, A., Chue, J. & Smith, C. A. Just how conserved is vertebrate sex determination? *Dev. Dyn.* **242**, 380–387 (2013).
- Piferrer, F. et al. The model of the conserved epigenetic regulation of sex. *Front. Genet.* **10**, 857 (2019).
- Herpin, A. & Scharlt, M. Plasticity of gene-regulatory networks controlling sex determination: of masters, slaves, usual suspects, newcomers, and usurpaters. *EMBO Rep.* **16**, 1260–1274 (2015).
- Li, J. & Ge, W. Zebrafish as a model for studying ovarian development: recent advances from targeted gene knockout studies. *Mol. Cell Endocrinol.* **507**, 110778 (2020).
- Lin, Y. T. & Capel, B. Cell fate commitment during mammalian sex determination. *Curr. Opin. Genet. Dev.* **32**, 144–152 (2015).
- Eggers, S., Ohnesorg, T. & Sinclair, A. Genetic regulation of mammalian gonad development. *Nat. Rev. Endocrinol.* **10**, 673–683 (2014).
- Niu, W. & Spradling, A. C. Two distinct pathways of pregranulosa cell differentiation support follicle formation in the mouse ovary. *Proc. Natl Acad. Sci. USA* **117**, 20015–20026 (2020).
- She, Z. Y. & Yang, W. X. Sry and Sox9 genes: How they participate in mammalian sex determination and gonadal development? *Semin. Cell Dev. Biol.* <https://doi.org/10.1016/j.semcdb.2016.07.032> (2016).
- Siegfried, K. R. & Nusslein-Volhard, C. Germ line control of female sex determination in zebrafish. *Dev. Biol.* **324**, 277–287 (2008).
- Slanchev, K., Stebler, J., de la Cueva-Mendez, G. & Raz, E. Development without germ cells: the role of the germ line in zebrafish sex differentiation. *Proc Natl Acad Sci USA* **102**, 4074–4079 (2005).
- Kurokawa, H. et al. Germ cells are essential for sexual dimorphism in the medaka gonad. *Proc. Natl. Acad. Sci. USA* **104**, 16958–16963 (2007).
- Nishimura, T. et al. Germ cells in the teleost fish medaka have an inherent feminizing effect. *PLoS Genet.* **14**, e1007259 (2018).
- Nishimura, T. et al. *foxl3* is a germ cell-intrinsic factor involved in sperm-egg fate decision in medaka. *Science* **349**, 328–331 (2015).
- Marques, I. J., Lupi, E. & Mercader, N. Model systems for regeneration: zebrafish. *Development* **146**, <https://doi.org/10.1242/dev.167692> (2019).
- Song, W. et al. Genetic evidence for estrogenicity of bisphenol A in zebrafish gonadal differentiation and its signalling mechanism. *J. Hazard Mater.* **386**, 121886 (2020).
- Lieschke, G. J. & Currie, P. D. Animal models of human disease: zebrafish swim into view. *Nat. Rev. Genet.* **8**, 353–367 (2007).

19. Sinclair, A. H. et al. A gene from the human sex-determining region encodes a protein with homology to a conserved DNA-binding motif. *Nature* **346**, 240–244 (1990).
20. Berta, P. et al. Genetic evidence equating SRY and the testis-determining factor. *Nature* **348**, 448–450 (1990).
21. Nanda, I. et al. A duplicated copy of DMRT1 in the sex-determining region of the Y chromosome of the medaka, *Oryzias latipes*. *Proc. Natl Acad. Sci. USA* **99**, 11778–11783 (2002).
22. Matsuda, M. et al. DMY is a Y-specific DM-domain gene required for male development in the medaka fish. *Nature* **417**, 559–563 (2002).
23. Li, M. et al. A tandem duplicate of anti-Müllerian hormone with a missense SNP on the Y chromosome is essential for male sex determination in Nile tilapia, *Oreochromis niloticus*. *PLoS Genet.* **11**, e1005678 (2015).
24. Liew, W. C. & Orban, L. Zebrafish sex: a complicated affair. *Brief Funct. Genomics* **13**, 172–187 (2014).
25. Liew, W. C. et al. Polygenic sex determination system in zebrafish. *PLoS ONE* **7**, e34397 (2012).
26. Rajkovic, A., Pangas, S. A., Ballow, D., Suzumori, N. & Matzuk, M. M. NOBOX deficiency disrupts early folliculogenesis and oocyte-specific gene expression. *Science* **305**, 1157–1159 (2004).
27. Kikuchi, M., Nishimura, T., Ishishita, S., Matsuda, Y. & Tanaka, M. foxl3, a sexual switch in germ cells, initiates two independent molecular pathways for commitment to oogenesis in medaka. *Proc. Natl Acad. Sci. USA* **117**, 12174–12181 (2020).
28. Hu, W., Gauthier, L., Baibakov, B., Jimenez-Movilla, M. & Dean, J. FIGLA, a basic helix-loop-helix transcription factor, balances sexually dimorphic gene expression in postnatal oocytes. *Mol. Cell Biol.* **30**, 3661–3671 (2010).
29. Liang, L., Soyal, S. M. & Dean, J. FIGa, a germ cell specific transcription factor involved in the coordinate expression of the zona pellucida genes. *Development* **124**, 4939–4947 (1997).
30. Soyal, S. M., Amleh, A. & Dean, J. FIGa, a germ cell-specific transcription factor required for ovarian follicle formation. *Development* **127**, 4645–4654 (2000).
31. Suzumori, N., Yan, C., Matzuk, M. M. & Rajkovic, A. Nobox is a homeobox-encoding gene preferentially expressed in primordial and growing oocytes. *Mech. Dev.* **111**, 137–141 (2002).
32. Lechowska, A. et al. Premature ovarian failure in nobox-deficient mice is caused by defects in somatic cell invasion and germ cell cyst breakdown. *J. Assist. Reprod. Genet.* **28**, 583–589 (2011).
33. Huntriss, J., Hinkins, M. & Pictou, H. M. cDNA cloning and expression of the human NOBOX gene in oocytes and ovarian follicles. *Mol. Hum. Reprod.* **12**, 283–289 (2006).
34. Qin, M. et al. Roles of figla/figla in juvenile ovary development and follicle formation during zebrafish gonadogenesis. *Endocrinology* **159**, 3699–3722 (2018).
35. Qin, M., Xie, Q., Wu, K., Zhou, X. & Ge, W. Loss of Nobox prevents ovarian differentiation from juvenile ovaries in zebrafish. *Biol. Reprod.* **106**, 1254–1266 (2022).
36. Wu, K., Song, W., Zhang, Z. & Ge, W. Disruption of dmrt1 rescues the all-male phenotype of the cyp19a1a mutant in zebrafish - a novel insight into the roles of aromatase/estrogens in gonadal differentiation and early folliculogenesis. *Development* **147**, dev182758 (2020).
37. Simpson, E. R. et al. Aromatase cytochrome P450, the enzyme responsible for estrogen biosynthesis. *Endocr. Rev.* **15**, 342–355 (1994).
38. Nakamura, M., Bhandari, R. K. & Higa, M. The role estrogens play in sex differentiation and sex changes of fish. *Fish Physiol. Biochem.* **28**, 113–117 (2003).
39. Matson, C. K. & Zarkower, D. Sex and the singular DM domain: insights into sexual regulation, evolution and plasticity. *Nat. Rev. Genet.* **13**, 163–174 (2012).
40. Webster, K. A. et al. Dmrt1 is necessary for male sexual development in zebrafish. *Dev. Biol.* **422**, 33–46 (2017).
41. Lin, Q. et al. Distinct and cooperative roles of amh and dmrt1 in self-renewal and differentiation of male germ cells in zebrafish. *Genetics* **207**, 1007–1022 (2017).
42. Lau, E. S., Zhang, Z., Qin, M. & Ge, W. Knockout of zebrafish ovarian aromatase gene (cyp19a1a) by TALEN and CRISPR/Cas9 leads to all-male offspring due to failed ovarian differentiation. *Sci Rep* **6**, 37357 (2016).
43. Yin, Y. et al. Targeted disruption of aromatase reveals dual functions of cyp19a1a during sex differentiation in zebrafish. *Endocrinology* **158**, 3030–3041 (2017).
44. Wang, C., Zhou, B. & Xia, G. Mechanisms controlling germline cyst breakdown and primordial follicle formation. *Cell. Mol. Life Sci.* **74**, 2547–2566 (2017).
45. Nagahama, Y. & Yamashita, M. Regulation of oocyte maturation in fish. *Dev. Growth Differ.* **50**, S195–S219 (2008).
46. Lubzens, E., Young, G., Bobe, J. & Cerdà, J. Oogenesis in teleosts: how fish eggs are formed. *Gen. Comp. Endocrinol.* **165**, 367–389 (2010).
47. Brion, F. et al. Impacts of 17 $\beta$ -estradiol, including environmentally relevant concentrations, on reproduction after exposure during embryo-larval-, juvenile- and adult-life stages in zebrafish (*Danio rerio*). *Aquat. Toxicol.* **68**, 193–217 (2004).
48. Zhang, Q. F. et al. Zebrafish *cyp11c1* knockout reveals the roles of 11-ketotestosterone and cortisol in sexual development and reproduction. *Endocrinology* **161**, <https://doi.org/10.1210/endo/bqaa048> (2020).
49. Liu, Y. et al. Single-cell transcriptome reveals insights into the development and function of the zebrafish ovary. *eLife* **11**, e76014 (2022).
50. Hiramatsu, N. et al. Ovarian yolk formation in fishes: molecular mechanisms underlying formation of lipid droplets and vitellogenin-derived yolk proteins. *Gen Comp Endocrinol* **221**, 9–15 (2015).
51. Chen, W., Lau, S. W., Fan, Y., Wu, R. S. S. & Ge, W. Juvenile exposure to bisphenol A promotes ovarian differentiation but suppresses its growth—potential involvement of pituitary follicle-stimulating hormone. *Aquat Toxicol* **193**, 111–121 (2017).
52. Zhai, Y. et al. Rescue of bmp15 deficiency in zebrafish by mutation of inha reveals mechanisms of BMP15 regulation of folliculogenesis. *PLoS Genet.* **19**, e1010954 (2023).
53. Pask, A. J. A role for estrogen in somatic cell fate of the mammalian gonad. *Chromosome Res.* **20**, 239–245 (2012).
54. Otsuka, F., McTavish, K. J. & Shimasaki, S. Integral role of GDF-9 and BMP-15 in ovarian function. *Mol. Reprod. Dev.* **78**, 9–21 (2011).
55. Bayne, R. A. et al. GDF9 is transiently expressed in oocytes before follicle formation in the human fetal ovary and is regulated by a novel NOBOX transcript. *PLoS ONE* **10**, e0119819 (2015).
56. Choi, Y. & Rajkovic, A. Characterization of NOBOX DNA binding specificity and its regulation of Gdf9 and Pou5f1 promoters. *J. Biol. Chem.* **281**, 35747–35756 (2006).
57. Zhao, L. et al. Rac1 modulates the formation of primordial follicles by facilitating STAT3-directed Jagged1, GDF9 and BMP15 transcription in mice. *Sci. Rep.* **6**, 23972 (2016).
58. Dranow, D. B. et al. Bmp15 is an oocyte-produced signal required for maintenance of the adult female sexual phenotype in zebrafish. *PLoS Genet.* **12**, e1006323 (2016).
59. Matson, C. K. et al. DMRT1 prevents female reprogramming in the postnatal mammalian testis. *Nature* **476**, 101–104 (2011).
60. Takahashi, H. Juvenile hermaphroditism in the zebrafish, *Brachydanio rerio*. *Bull. Fac. Fish Hokkaido Univ.* **28**, 57–65 (1977).
61. Selman, K., Wallace, R. A., Sarka, A. & Qi, X. P. Stages of oocyte development in the zebrafish, *Brachydanio rerio*. *J. Morphol.* **218**, 203–224 (1993).
62. Zheng, P. & Dean, J. Oocyte-specific genes affect folliculogenesis, fertilization, and early development. *Semin. Reprod. Med.* **25**, 243–251 (2007).
63. Pangas, S. A. & Rajkovic, A. Transcriptional regulation of early oogenesis: in search of masters. *Hum. Reprod. Update* **12**, 65–76 (2006).
64. Wang, Z. P., Liu, C. Y., Zhao, Y. G. & Dean, J. FIGLA, LHX8 and SOHLH1 transcription factor networks regulate mouse oocyte growth and differentiation. *Nucleic Acids Res.* **48**, 3525–3541 (2020).
65. Chen, W. et al. Loss of growth differentiation factor 9 causes an arrest of early folliculogenesis in zebrafish—a novel insight into its action mechanism. *PLoS Genet.* **18**, e1010318 (2022).
66. Zhang, Z., Wu, K., Ren, Z. & Ge, W. Genetic evidence for Amh modulation of gonadotropin actions to control gonadal homeostasis and gametogenesis in zebrafish and its noncanonical signaling through Bmpr2a receptor. *Development* **147**, dev189811 (2020).
67. Sanfins, A., Rodrigues, P. & Albertini, D. F. GDF-9 and BMP-15 direct the follicle symphony. *J. Assist. Reprod. Genet.* **35**, 1741–1750 (2018).
68. Zhang, Z., Zhu, B. & Ge, W. Genetic analysis of zebrafish gonadotropin (FSH and LH) functions by TALEN-mediated gene disruption. *Mol. Endocrinol.* **29**, 76–98 (2015).
69. Wang, Y. & Ge, W. Developmental profiles of activin  $\beta$ A,  $\beta$ B, and follistatin expression in the zebrafish ovary: evidence for their differential roles during sexual maturation and ovulatory cycle. *Biol. Reprod.* **71**, 2056–2064 (2004).
70. Chen, W. & Ge, W. Gonad differentiation and puberty onset in the zebrafish: evidence for the dependence of puberty onset on body growth but not age in females. *Mol. Reprod. Dev.* **80**, 384–392 (2013).
71. Zhou, R., Tsang, A. H., Lau, S. W. & Ge, W. Pituitary adenylate cyclase-activating polypeptide (PACAP) and its receptors in the zebrafish ovary: evidence for potentially dual roles of PACAP in controlling final oocyte maturation. *Biol. Reprod.* **85**, 615–625 (2011).
72. Li, C. W. & Ge, W. Spatiotemporal expression of bone morphogenetic protein family ligands and receptors in the zebrafish ovary: a potential paracrine signaling mechanism for oocyte-follicle cell communication. *Biol. Reprod.* **85**, 977–986 (2011).
73. Brion, F. et al. Impacts of 17 beta-estradiol, including environmentally relevant concentrations, on reproduction after exposure during embryolarval-, juvenile- and adult-life stages in zebrafish (*Danio rerio*). *Aquatic Toxicol.* **68**, 193–217 (2004).

74. Zhu, B., Pardeshi, L., Chen, Y. & Ge, W. Transcriptomic analysis for differentially expressed genes in ovarian follicle activation in the zebrafish. *Front. Endocrinol. (Lausanne)* **9**, 593 (2018).

### Acknowledgements

The authors thank Ms. Phoenix Un Ian LEI for the maintenance and management of the zebrafish facility and the Histology Core of the Faculty of Health Sciences for technical support. This study was supported by grants from the University of Macau (MYRG2020-00192-FHS, MYRG2022-00219-FHS and CPG2023-00029-FHS) and The Macau Fund for Development of Science and Technology (FDCT0132/2019/A3 and FDCT0086/2022/AFJ) to W.G. K.W. is supported by the Natural Science Foundation of Guangdong Province, China (2022A1515110089), the open competition program of top ten critical priorities of Agricultural Science and Technology Innovation for the 14th Five-Year Plan of Guangdong Province (NO.2022SDZG01) and the Macau Young Scholars Program (AM2020025).

### Author contributions

W.G. developed the hypothesis, designed the experiments, revised the manuscript, supervised and administered the project. K.W. performed most of the experiments, analyzed data, prepared figures, and drafted the manuscript. Y.Z. developed the method for E2 oral administration and performed E2 treatment. M.Q. generated the *figla*<sup>-/-</sup> and *nobox*<sup>-/-</sup> mutants. C.Z., N.A., and J.H. helped with the laboratory work. All authors approved the final manuscript.

### Competing interests

The authors declare no competing interests.

### Additional information

**Supplementary information** The online version contains supplementary material available at <https://doi.org/10.1038/s42003-023-05551-1>.

**Correspondence** and requests for materials should be addressed to Wei Ge.

**Peer review information** *Communications Biology* thanks Juan (I) Fernandino, Mariko Kikuchi and the other, anonymous, reviewer(s) for their contribution to the peer review of this work. Primary Handling Editor: George Inglis.

**Reprints and permission information** is available at <http://www.nature.com/reprints>

**Publisher's note** Springer Nature remains neutral with regard to jurisdictional claims in published maps and institutional affiliations.



**Open Access** This article is licensed under a Creative Commons Attribution 4.0 International License, which permits use, sharing, adaptation, distribution and reproduction in any medium or format, as long as you give appropriate credit to the original author(s) and the source, provide a link to the Creative Commons license, and indicate if changes were made. The images or other third party material in this article are included in the article's Creative Commons license, unless indicated otherwise in a credit line to the material. If material is not included in the article's Creative Commons license and your intended use is not permitted by statutory regulation or exceeds the permitted use, you will need to obtain permission directly from the copyright holder. To view a copy of this license, visit <http://creativecommons.org/licenses/by/4.0/>.

© The Author(s) 2023, corrected publication 2023